ACS OMEGA

Open Access

This article is licensed under CC-BY-NC-ND 4.0

http://pubs.acs.org/journal/acsodf

Article

Discovery of PRMT5 N-Terminal TIM Barrel Ligands from Machine-Learning-Based Virtual Screening

Zhihang Shen, Gustavo Seabra, Jason Brant, Kalyanee Shirlekar, Loic Deleyrolle, Benjamin Lewis, and Chenglong Li*

Cite This: *ACS Omega* 2025, 10, 1156−1163

Read Online

ACCESS | Metrics & More | Article Recommendations | Supporting Information

ABSTRACT: Protein arginine methyltransferase 5 (PRMT5), which symmetrically dimethylates cytosolic and nuclear proteins, has been demonstrated as an important cancer therapeutic target. In recent years, many advanced achievements in PRMT5 inhibitor development have been made. Most PRMT5 inhibitors in the clinical trial focus on targeting the C-terminal catalytic domain, whereas developing small molecules to interrupt the PRMT5/pICLn (methylosome subunit) protein−protein interface is also of great importance for inhibiting PRMT5. Here, we describe a machine-learning-based virtual screening method and use this novel pipeline to screen small-molecule inhibitors of the PRMT5/pICLn interaction. 18 compounds were manually selected for experimental testing. One compound, Z319334062, showed surface plasmon resonance-binding affinity to the target (K_D = 21.5 μM) and dose-dependently inhibited symmetric dimethylation levels in patient-derived glioblastoma cell lines.

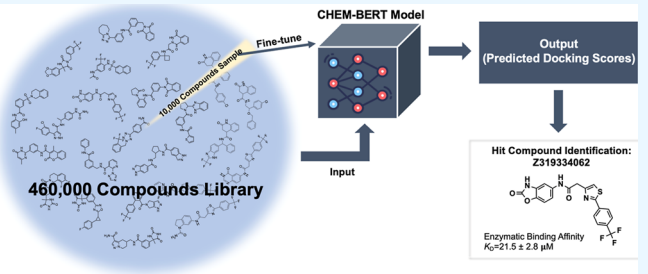

INTRODUCTION

Protein arginine methyltransferases (PRMTs), a family of proteins that methylate arginine residues in both histone and nonhistone proteins, are among the most important methylation enzymes. These methylation events regulate transcription,[1] RNA splicing,[2] DNA repair, cell cycle,[3] hormone-receptor signaling,[4] and the immune response.[5] PRMT5, a type II PRMT enzyme, utilizes the cofactor *S*-adenosylmethionine (SAM) as a methyl donor to symmetrically dimethylate the protein arginine guanidinium nitrogen, generating a methylated guanidinium moiety and *S*-adenosylhomocysteine, which is salvaged and reused for methionine biosynthesis. Clinical and preclinical studies have shown that increased PRMT5 expression directly correlates with poor cancer prognosis and survival rate.[6] Thus, the development of PRMT5 inhibitors is of great importance.

Currently, most PRMT5 inhibitors in clinical trials focus on targeting the C-terminal catalytic domain and can be classified as SAM-competitive,[7−13] substrate-competitive,[14−17] or MTA-cooperative inhibitors[18−28] (Figures 1 and 2). However, a new interface between the PRMT5 N-terminal TIM Barrel Motif (PBM) and its substrate adaptor proteins (pICLn, Riok1, and COPR5) was recently revealed by McKinney et al.[29,30] This PBM-SAPs interaction is required for recruiting specific substrates, including histone and spliceosome complexes, to the PRMT5 methylation site.[31] Two lead compounds, a covalent inhibitor (BRD0639) and a cyclic peptide (peptide50), were developed to interrupt this interaction.[29,32] Both molecules showed biochemical and on-target cellular activity that supports the exploration of a new class of PRMT5 inhibitors.

Meanwhile, Beketova et al. demonstrated that inhibiting PRMT5/pICln interaction can avoid the androgen receptor (AR) and AR splice variant reactivation in the castration-resistant prostate cancer (CRPC), which provided a novel perspective in CRPC treatment.[33] Following the previous mechanism studies, a cryo-EM structure with full-length PRMT5:MEP50 and pICLn was resolved (unpublished results). Although most residues were unclear due to the high flexibility of pICLn, residues 205−234 were found to be clearly bound to the PRMT5 N-terminal TIM barrel domain. Surprisingly, a secondary binding pocket was discovered (Figure 3a). Based on the cryo-EM structure, the short loop of $pICLn_{205-213}$ formed a network of van der Waals and hydrogen bond interactions with PRMT5. The hydrophobic side chain of Ile211 of pICLn snugly fits into a hydrophobic pocket composed of side chains of Phe40, Val83, Pro120, Ala121, and Trp152 of PRMT5 (Figure 3b). Unlike the PBM site's flat surface and shallow groove, this newly defined pocket is more hydrophobic with a deeper pocket for noncovalent small-molecule inhibitors to bind. Therefore, in this study, we

Received: September 20, 2024
Revised: December 12, 2024
Accepted: December 17, 2024
Published: January 2, 2025

© 2025 The Authors. Published by American Chemical Society

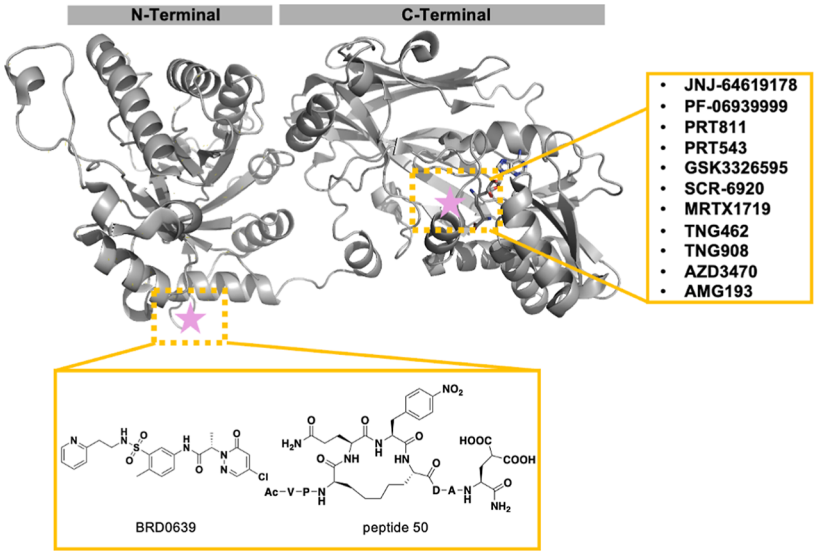

Figure 1. PRMT5 monomer structure overview and current ligands binding to the N-terminal or C-terminal. The gray cartoon shows the overall structure of PRMT5. Pink stars indicates the binding site of ligands. The two ligands in the yellow box bind to the PRMT5 N-terminal PBM site. 11 ligands that bind to the C-terminal catalytic site are in clinical trials.

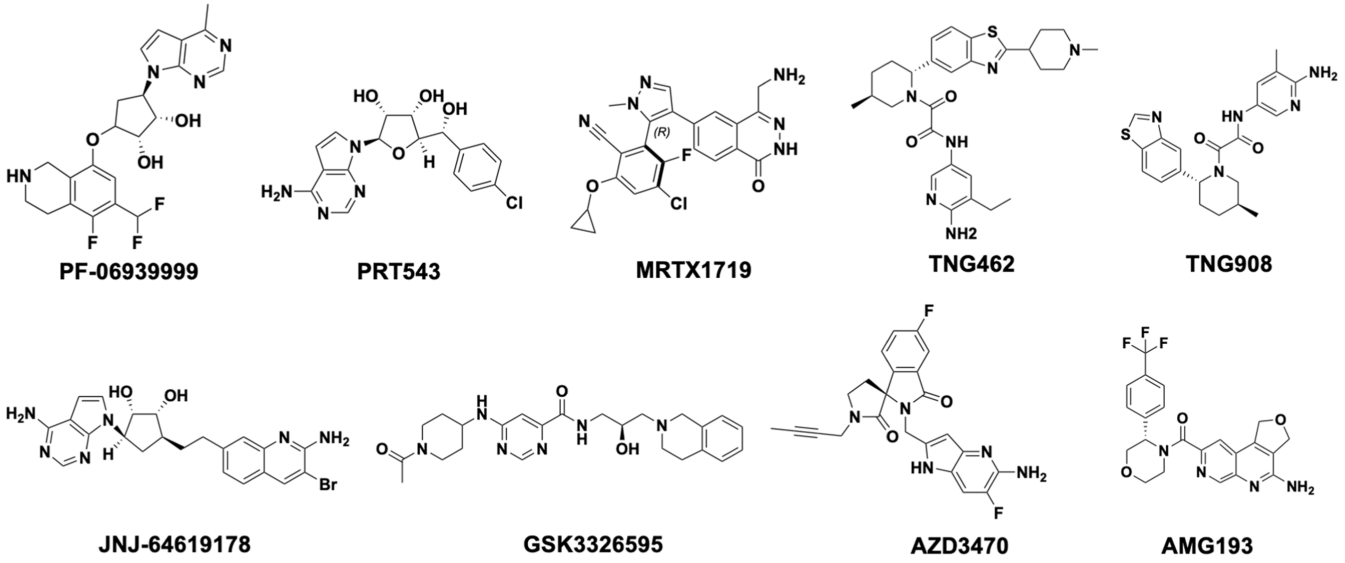

Figure 2. PRMT5 inhibitors in clinical trials.

aimed to utilize a machine-learning-based virtual screening pipeline to identify ligands that disrupt PRMT5/pICLn interactions by targeting this newly defined pocket.

RESULTS AND DISCUSSION

In this study, to further validate the key residues of the hydrophobic pocket, a per-residue binding energy decomposition calculation was performed by MMPBSA to estimate the binding energy contribution of single residues in the system. We first manually truncated the $(PRMT5)_4(MEP50)_4(pICLn)_4$ cryo-EM structure, keeping only the PRMT5 N-terminal TIM barrel (residues 1−292) and pICLn (residues 205−234), and then ran a 200 ns MD simulation with the truncated structure. Two clusters of residues in the pICLn (residues 205−234) peptide contributed most to the whole binding interactions: Ile211 and Arg212 from the newly defined site; Gln228, Phe229, and Glu230 from the PBM site (Figure 3c). Thus, besides the PBM site, $pICLn_{205-213}$ was also involved in the PRMT5/pICLn interaction, consistent with the results of Krzyzanowski et al.[31]

After validating the ligand-binding site, we applied a machine-learning-based virtual screening method (Figure 4) to screen small-molecule inhibitors binding to this newly defined pocket. First, we randomly selected 10,000 diverse compounds from Enamine HLL-460 Compound Library (460 K) and docked those compounds into the pocket using AutoDock Vina.[34] These data were used to fine-tune the CHEM-BERT model[35] to predict docking scores from the SMILES strings of compounds (Figure S1a,b). After that, the whole Enamine HLL-460 Compound Library (460,000 compounds) was scanned with the fine-tuned model (Figure S1c), and then 10,000 compounds with the best-predicted scores were docked with AutoDock Vina again to obtain actual docking scores. To evaluate the model prediction accuracy, the correlation between vina scores and prediction scores in the set of selected top 10,000 molecules was shown (Figure S1d).

https://doi.org/10.1021/acsomega.4c08661
ACS Omega 2025, 10, 1156−1163

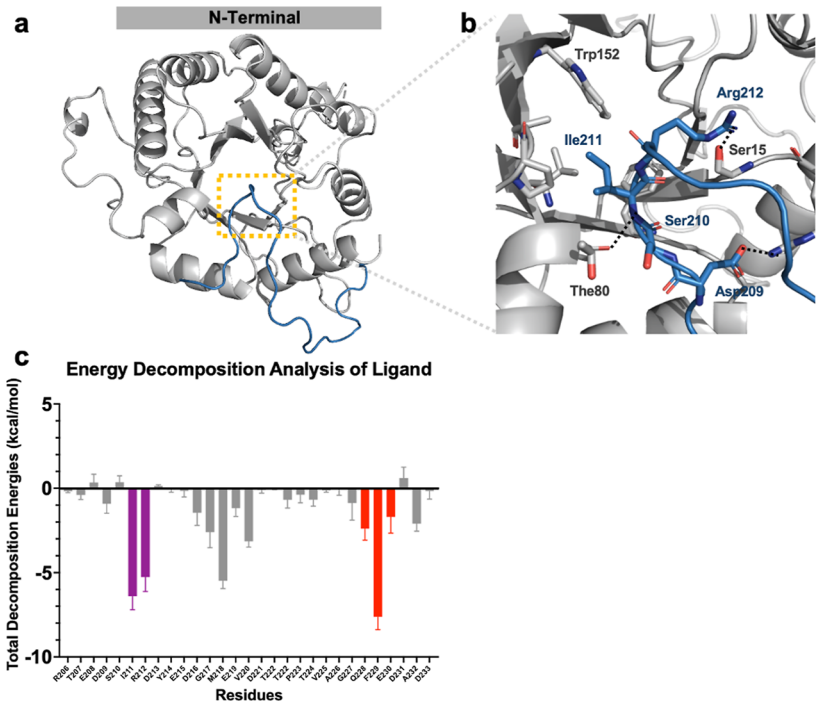

Figure 3. Interaction between PRMT5 N-terminal (1−292) and pICLn (205−234). (a) Cryo-EM structure of PRMT5 N-terminal (1−292) and pICLn (205−234). (b) Interactions between PRMT5 and pICLn around newly defined binding sites. Hydrogen bonds are shown in black dotted lines. The Ile211 of pICLn is inserted into a hydrophobic pocket composed of Phe40, Val83, Pro120, Ala121, and Trp152 of PRMT5. (c) MMPBSA free-energy decomposition calculation.

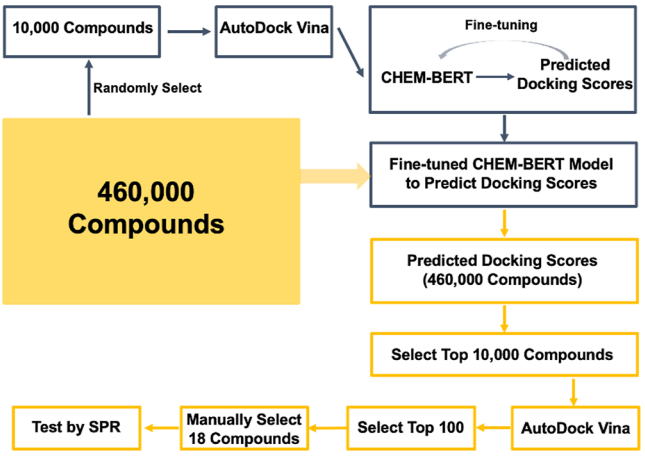

Figure 4. Machine-learning-based virtual screening pipeline.

18 compounds were selected through visual inspection of the docking modes from the compound list with the top 100 docking scores (Figure S2). Of those, seven compounds did not show any surface plasmon resonance (SPR)-binding signal, 10 compounds showed nonspecific interactions, and one compound, Z319334062, showed specific-binding affinity (K_D = 21.5 μM) to the PRMT5 N-terminal TIM barrel domain (Figure 5a,b). The Vina Score of Z319334062 is −8.1 kcal/mol. Meanwhile, a 200 ns MD simulation was run to visualize the interaction details. The benzo[*d*]oxazol-2(3*H*)-one formed two hydrogen bonds with the Pro120 main chain and the Trp152 side chain to stabilize the binding on one side of the molecule (Figure S3), whereas the (trifluoromethyl)benzene on the other side was inserted into the hydrophobic pocket composed of side chains of Phe40, Val83, Pro120, Ala121, and Trp152. The amide bond and thiazole in the middle act as linkers to connect the two parts (Figure 5c). The binding energy estimated with MM-PBSA without entropy calculation was −8.7 ± 3 kcal/mol.

To determine which cell lines to test the compound cellular activity, RNA-Seq data from six tumor types were analyzed, and only glioblastoma (GBM) was found with a higher expression level of PRMT5 and pICLn in tumor tissue (Figure S4a). Thus, to evaluate whether Z319334062 could disrupt PRMT5/pICln interaction in a cellular context, two patient-derived glioblastoma (GBM) cell lines, L1 and R24−03, with differentially expressed PRMT5 and CLNS1A levels, were selected (Figure S4b). In the cell viability assay, after 4 day treatment, the IC_{50} in L1 (IC_{50} = 12.8 μM) was significantly lower than that in R24−03 (IC_{50} = 51.0 μM), indicating higher drug sensitivity in PRMT5/CLNS1A overexpressed cell line (Figure 6a). In addition, cellular treatment with Z319334062 and GSK3326595 (positive control) resulted in inhibition of PRMT5 methyltransferase function, as demonstrated by the reduction in symmetric dimethylated arginine (SDMA) level by Western Blot (Figures 6b and S4c). We found that some substrates but not all were inhibited by the treatment of Z319334062. This finding was consistent with the data published by McKinney et al.[30] Finally, to test if Z319334062 was able to disrupt the interaction between PRMT5 and pICLn in L1 cells, we used a coimmunoprecipitation assay. Under 40 μM Z319334062 treatment, we found that the PRMT5/pICLn complex was disrupted compared to the negative control (Figure 6c). In the meantime, we found that the PRMT5 melting temperature was significantly shifted under 25 μM Z319334062 treatment for 18 h (Figure 6d).

https://doi.org/10.1021/acsomega.4c08661
ACS Omega 2025, 10, 1156−1163

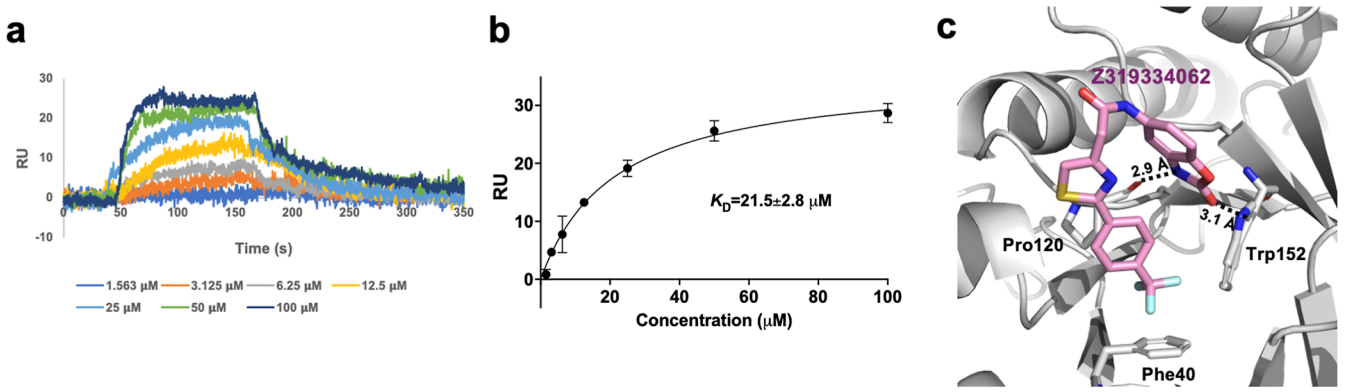

Figure 5. Biochemical, cellular, and computational evaluation of Z319334062. (a) SPR-binding sensorgram under different concentrations of Z319334062. (b) Binding affinity (K_D) evaluation by SPR. (c) One snapshot from 200 ns MD simulation showed the binding interactions between Z319334062 and PRMT5 N-terminal.

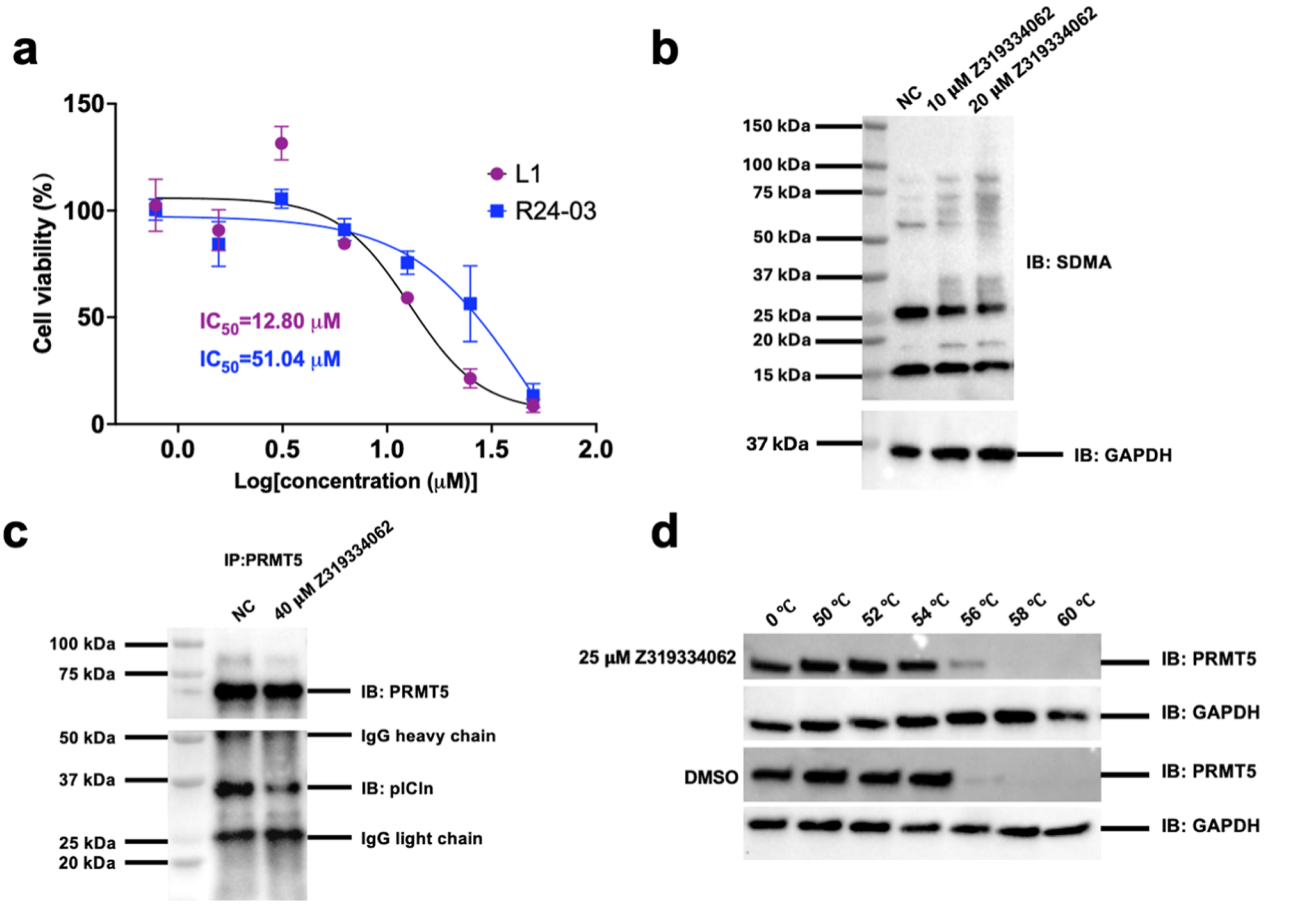

Figure 6. (a) Cell viability comparison of L1 and R24−03 cell lines under four-day treatment. (b) After drug treatments, the SDMA level of L1 downregulated dose-dependently. (c) 40 μM Z319334062 disrupted PRMT5/pICLn interaction in L1 cell line under four-day treatment. (d) 25 μM Z319334062 shifted PRMT5 melting temperature about 1 °C under 18 h treatment.

CONCLUSIONS

We applied an ML-based in silico virtual screening method to identify potential PRMT5 N-terminal TIM barrel-binding ligands, followed by biochemical screening of 18 potential inhibitors. Of them, one was considered a promising noncovalent PRMT5/pICLn inhibitor. In this screening, the efficiency improved by approximately 96%. Specifically, with the ML-based pipeline, only 20,000 compounds (in total with 39,090 variants = 22,191 variants for training + 16,889 variants for selected compounds) needed to be docked. In comparison, docking the entire library would require processing 460,000 compounds (in total with 867,859 variants). Also, the hit rate of 5.6% is modest but marks a significant improvement compared to the less than 1% hit rate typically seen in high-throughput screening.[36] Since the N-terminal domain of PRMT5 is a newly identified drug binding site, only two inhibitors were reported to bind to it. One is a covalent binder, BRD0639 (K_D = 13.8 μM),[29] and the other is a cyclic peptide, Peptide50 (K_D = 89 ± 11 nM),[31] both of which were discovered following multiple rounds of optimization. In

https://doi.org/10.1021/acsomega.4c08661
ACS Omega 2025, 10, 1156−1163

contrast, our lead compound demonstrates a binding affinity of around 20 μM, achieved solely through machine-learning-based virtual screening without any optimization, highlighting its significant potential.

To visualize the binding, we ran a 200 ns MD simulation of the active compound, Z319334062, bound to the TIM barrel domain to analyze the binding mode for further structure−activity relationship optimization. Moreover, we selected two representative GBM cell lines by a The Cancer Genome Atlas (TCGA) database screening for cellular investigation. The results indicated that Z319334062 was much more effective in the PRMT5/CLNS1A overexpressed cell line under dose-dependent treatment. In addition, Z319334062 was also able to disrupt the PRMT5/pICLn interaction at the cellular level. These evidences suggested that Z319334062 may be a lead compound for designing more potent analogues for novel cancer therapeutics.

METHODS

TCGA Screening. RNA-Seq data from TCGA was downloaded using the Genomic Data Commons portal, focusing on six tumor types: glioblastomas (GBM), invasive breast cancer, lung adenocarcinoma, prostate adenocarcinoma, pancreatic adenocarcinoma, and diffuse large B-cell lymphoma (DLBCL). The data included both tumor and normal tissue samples for five tumor types (except DLBCL). The RSEM counts were preprocessed to remove outliers, filtered to remove lowly expressed genes, and normalized, and differential gene expression analysis was performed on the five solid tumors, using the "TCGAbiolinks" package in R. The genes of interest, PRMT5, and CLNS1A were found differentially expressed in glioblastoma samples (filtering criteria used: FDR = 0.01, log FC = 1).

PRMT5 N-Terminal TIM Barrel Protein Expression, Purification, and Characterization. pT7-FLAG-His-TIM plasmid was expressed in BL21 competent *E. coli* (New England Biolabs, #C2530H). The overnight culture was harvested and lysed by sonication in wash buffer (20 mM Tris−HCl, 8 M urea, 500 mM NaCl, 5 mM imidazole, 1 mM DTT, pH = 8.0). After the removal of cell debris, supernatants were filtered by 0.22 μm filter (Sigma-Aldrich, #SLGPM33RS) and then loaded to HisTrap HP His tag protein purification columns (Cytiva, #29051021), followed by gradient elution (20 mM Tris−HCl, 8 M urea, 500 mM NaCl, 500 mM imidazole, 1 mM DTT, pH = 8.0). The elution product was dialyzed in refolding buffer (20 mM Tris−HCl, 5% glycerol, 500 mM NaCl, 5 mM DTT, 1 mM EDTA, 0.05% P20, pH = 8.0) and then desalted by PD-10 desalting columns (Cytiva, #17085101). The desalting sample was concentrated to 2 mg/mL in storage buffer (10 mM HEPES, 50 mM NaCl, 10% (v/v) glycerol, 2 mM DTT, pH 8.0) and was stored at −80 °C until the time of use.

Surface Plasmon Resonance-Binding Study. Binding affinity measurements were conducted on a Reichert2SPR instrument (Ametek) at room temperature. 10 mg of PRMT5 N-terminal TIM barrel protein was directly immobilized onto the 500,000 Da carboxymethyl dextran sensor chip at pH 5.5 using the standard amine coupling approach. Small-molecule ligands were injected at a flow rate of 30 mL/min at different concentrations in the running buffer (10 mM HEPES at pH 7.4, 150 mM NaCl, 3 mM EDTA, 0.005% v/v Tween-20, and 5% DMSO). The association and dissociation time were 2 and 5 min, respectively. Sensorgram data were processed using Excel, and dissociation constant (K_D) was calculated by GraphPad Prism9.

Compounds. All compounds were purchased from Enamine, and their purity, as tested in the biological assay, was confirmed to be >95%.

Cell Culture. L1 and R24−03 patient-derived cells were maintained in Neurocult NS-A Basal Medium plus 10% Human NeuroCult NS-A Proliferation Supplements (StemCell Technologies, #05751). Recombinant human epidermal growth factor (R&D Systems, #236-EG), recombinant human basic fibroblast growth factor (R&D Systems, #233-FB/CF), heparin (Sigma-Aldrich, #H3149), and antibiotic antimycotic solution 100′ (Corning, #30-004-Cl) are supplemented in the medium.[37] The cell suspension was taken from the flask and spun down at 500 g for 5 min. Then, 1 mL of trypsin was added and the mixture incubated for 5−10 min at 37 °C. Neutralized by 3 mL of complete media, the mixture was spun down again. The cell number was resuspended and counted.

Antibodies. All primary antibodies were used in PBST buffer with 5% BSA: anti-SDMA (1:1000, Cell Signaling #13222S), anti-GAPDH (1:1000, Santa Cruz Biotechnology #sc-47724), anti-PRMT5 (1:1000, Cell Signaling #79998), anti-pICln (1:1000, Santa Cruz Biotechnology #sc-393,525), antirabbit IgG, HRP-linked Antibody (Cell Signaling #7074), and antimouse IgG, HRP-linked antibody (Cell Signaling #7076).

In Vitro Cell Viability. Cells were seeded into nontreated 96-well plates at a density of 3000 cells/well. Test compounds were then added into the cells at different concentrations and incubated for 96 h. 10 mL of the CCK8 cell counting reagent (MedChemExpress #HY-K0301) was added to each well and then incubated at 37 °C for another 4 h. The absorbance was determined at 562 nm by using a microplate reader.

Immunoblot and Immunoprecipitation. Cells were rinsed with ice-cold phosphate-buffered saline and lysed with IP lysis buffer (Pierce no. 87787) supplemented with protease and phosphatase inhibitor cocktail (Pierce #78441). The cell lysates were centrifuged at 13,000 rpm for 30 min at 4 °C. The protein concentrations were measured using a BCA protein assay kit (Pierce #23227). Equal amounts of whole cell lysates were resolved by SDS-polyacrylamide gel electrophoresis (SDS-PAGE) (Bio-Rad #4561086), transferred to a PVDF membrane (Bio-Rad #1620174), and then immunoblotted with the indicated antibodies. For immunoprecipitation, the lysates (100 μg) were incubated with 30 mL of protein A/G PLUS-agarose (SCBT #sc-2003) and corresponding primary antibodies at 4 °C overnight. The immunoprecipitation was then washed five times with IP lysis buffer before being resolved by SDS-PAGE. The membranes were analyzed by using ECL Western blotting detection reagents (Pierce no. 34096) and imaged with ChemiDoc MP imaging system (Bio-Rad).

Molecular Docking. The target (PDB: 7SER) was prepared using Schrödinger Protein Preparation Protocol at pH 7.4 ± 2.0, and water molecules with less than two hydrogen bonds to ligand atoms were deleted. Ligands were processed with Schrodinger Ligprep to generate three-dimensional structures from the SMILES strings, along with all possible protonation states and stereoisomers, resulting in 22,191 "variants". The grid box was centered on pICln (residues 205−234) with 14.0 Å in all directions. All dockings were carried out with AutoDock Vina 1.2 using exhaustiveness 32. Only the

https://doi.org/10.1021/acsomega.4c08661
ACS Omega 2025, 10, 1156−1163

best docking score for each molecule was considered in the analysis and ML model training.

Machine Learning Model. The SMILES strings and docking scores of the sample library were used to fine-tune the CHEM-BERT model.[35] The training set is split into three sets with proportions of 80:10:10 for training, validation, and testing. The model was trained for 14 epochs using only the training and validation sets, and the model obtained from epoch 4, with the lowest validation loss, was selected. The scores predicted on the holdout test set showed a correlation of r^2 = 0.77 with the actual Vina scores (ground truth), and this final model was used to predict Vina Scores for the entire library.

Molecular Dynamics Simulation. The initial structure of Z319334062 bound to PRMT5 N-terminus (1−292) was obtained from the virtual screening step. The system was placed in a truncated octahedral box with sides at least 20 Å from any solute atoms. The system was solvated with OPC waters,[38] charges were neutralized with Na^+ and Cl^- ions, and extra ions were added to reach a salt concentration of 0.15 M. The Amber ff19SB force field[39] was used for the protein atoms, and the Z319334062 ligand was represented with GAFF[40] force field. The system was then submitted to 100 steps of minimization where only the waters were allowed to move, followed by 10,000 minimization steps where all atoms were allowed to move. The system was heated at a constant volume for 0.6 ns to 310 K, followed by 0.4 ns relaxation at the final temperature. This was followed by a 2 ns relaxation at the final temperature and constant 1 atm pressure and a final 200 ns simulation with the same conditions.

Statistical Analysis. All experiments were performed in triplicate. As indicated in the figure legends, all quantitative data are presented as the mean ± SD or mean ± SEM of three biologically independent experiments or samples. Statistical significance was determined by a two-tailed Student's *t*-test or ANOVA test of variance. $P < 0.05$ was considered statistically significant.

■ ASSOCIATED CONTENT

Supporting Information

The Supporting Information is available free of charge at https://pubs.acs.org/doi/10.1021/acsomega.4c08661.

Chem-Bert model statistics; structures of purchased compounds; lead compound MD analysis; and Prmt5 and pICLn expression levels in tested cancer cell lines (PDF)

■ AUTHOR INFORMATION

Corresponding Author

Chenglong Li − *Department of Medicinal Chemistry, College of Pharmacy, University of Florida, Gainesville, Florida 32610, United States; UF Health Cancer Center, University of Florida, Gainesville, Florida 32610, United States;* orcid.org/0000-0001-9460-3168; Email: lic@cop.ufl.edu

Authors

Zhihang Shen − *Department of Medicinal Chemistry, College of Pharmacy, University of Florida, Gainesville, Florida 32610, United States;* orcid.org/0009-0003-2505-1680

Gustavo Seabra − *Department of Medicinal Chemistry, College of Pharmacy, University of Florida, Gainesville, Florida 32610, United States;* orcid.org/0000-0002-1303-4483

Jason Brant − *UF Health Cancer Center and Department of Biostatistics, College of Public Health and Health Professions & College of Medicine, University of Florida, Gainesville, Florida 32610, United States*

Kalyanee Shirlekar − *UF Health Cancer Center, University of Florida, Gainesville, Florida 32610, United States*

Loic Deleyrolle − *Department of Neurosurgery, College of Medicine, University of Florida, Gainesville, Florida 32610, United States; Department of Molecular Medicine, Mayo Clinic Florida, Jacksonville, Florida 32224, United States;* orcid.org/0000-0002-1129-744X

Benjamin Lewis − *Department of Medicinal Chemistry, College of Pharmacy, University of Florida, Gainesville, Florida 32610, United States*

Complete contact information is available at: https://pubs.acs.org/10.1021/acsomega.4c08661

Author Contributions

The manuscript was written through the contributions of all authors. All authors have given approval to the final version of the manuscript. Conceptualization, Z.S. and C.L.; formal analysis, Z.S., G.S., J.B., K.S., B.L., and C.L.; funding acquisition, C.L.; investigation, Z.S., G.S., J.B., K.S., L.D., B.L., and C.L.; methodology, Z.S., G.S., B.L., and C.L.; project administration, Z.S. and C.L.; supervision, Z.S., G.S., L.D., and C.L.; writing—original draft, Z.S.; and writing, review, and editing, Z.S., G.S., J.B., K.S., L.D., B.L., and C.L.

Notes

The authors declare no competing financial interest.

■ ACKNOWLEDGMENTS

Research reported in this publication was supported by the Bodor Professorship and R01CA212403 to C.L., the UF Health Cancer Center, supported in part by state appropriations provided in Fla. Stat. § 381.915, and the National Cancer Institute of the National Institutes of Health under award number P30CA247796. The content is solely the responsibility of the authors and does not necessarily represent the official views of the National Institutes of Health or the State of Florida. We gratefully thank Prof. Jorg Bungert (University of Florida) and Prof. Wenjian Gan (Medical University of South Carolina) for giving us pT7-FLAG-His and myc-PRMT5 plasmids, respectively.

■ ABBREVIATIONS

PRMT5, protein arginine methyltransferase 5; SDMA, symmetrically dimethylated arginines; SAM, *S*-adenosylmethionine; SAH, *S*-adenosylhomocysteine; MTA, methylthioadenosine; PBM, PRMT5 N-terminal TIM barrel motif; SAPs, substrate adaptor proteins; AR, androgen receptor; CRPC, castration-resistant prostate cancer; GBM, glioblastoma; HTS, high-throughput screening; SAR, structure−activity relationship; SPR, surface plasmon resonance; MD, molecular dynamics.

■ REFERENCES

(1) Majumder, S.; Alinari, L.; Roy, S.; Miller, T.; Datta, J.; Sif, S.; Baiocchi, R.; Jacob, S. T. Methylation of histone H3 and H4 by PRMT5 regulates ribosomal RNA gene transcription. *J. Cell. Biochem.* **2010**, *109* (3), 553−563.

(2) Hamard, P. J.; Santiago, G. E.; Liu, F.; Karl, D. L.; Martinez, C.; Man, N.; Mookhtiar, A. K.; Duffort, S.; Greenblatt, S.; Verdun, R. E.; Nimer, S. D. PRMT5 Regulates DNA Repair by Controlling the Alternative Splicing of Histone-Modifying Enzymes. *Cell Rep.* **2018**, *24* (10), 2643−2657.
(3) Jiang, H.; Zhu, Y.; Zhou, Z.; Xu, J.; Jin, S.; Xu, K.; Zhang, H.; Sun, Q.; Wang, J.; Xu, J. PRMT5 promotes cell proliferation by inhibiting BTG2 expression via the ERK signaling pathway in hepatocellular carcinoma. *Cancer Med.* **2018**, *7* (3), 869−882.
(4) Wang, S. M.; Dowhan, D. H.; Muscat, G. E. O. Epigenetic arginine methylation in breast cancer: emerging therapeutic strategies. *J. Mol. Endocrinol.* **2019**, *62* (3), R223−R237.
(5) Webb, L. M.; Sengupta, S.; Edell, C.; Piedra-Quintero, Z. L.; Amici, S. A.; Miranda, J. N.; Bevins, M.; Kennemer, A.; Laliotis, G.; Tsichlis, P. N.; Guerau-de-Arellano, M. Protein arginine methyltransferase 5 promotes cholesterol biosynthesis-mediated Th17 responses and autoimmunity. *J. Clin. Invest.* **2020**, *130* (4), 1683−1698.
(6) Vinet, M.; Suresh, S.; Maire, V.; Monchecourt, C.; Nemati, F.; Lesage, L.; Pierre, F.; Ye, M.; Lescure, A.; Brisson, A.; Meseure, D.; Nicolas, A.; Rigaill, G.; Marangoni, E.; Del Nery, E.; Roman-Roman, S.; Dubois, T. Protein arginine methyltransferase 5: A novel therapeutic target for triple-negative breast cancers. *Cancer Med.* **2019**, *8* (5), 2414−2428.
(7) Brehmer, D.; Beke, L.; Wu, T.; Millar, H. J.; Moy, C.; Sun, W.; Mannens, G.; Pande, V.; Boeckx, A.; van Heerde, E.; Nys, T.; Gustin, E. M.; Verbist, B.; Zhou, L.; Fan, Y.; Bhargava, V.; Safabakhsh, P.; Vinken, P.; Verhulst, T.; Gilbert, A.; Rai, S.; Graubert, T. A.; Pastore, F.; Fiore, D.; Gu, J.; Johnson, A.; Philippar, U.; Morschhauser, B.; Walker, D.; De Lange, D.; Keersmaekers, V.; Viellevoye, M.; Diels, G.; Schepens, W.; Thuring, J. W.; Meerpoel, L.; Packman, K.; Lorenzi, M. V.; Laquerre, S. Discovery and Pharmacological Characterization of JNJ-64619178, a Novel Small-Molecule Inhibitor of PRMT5 with Potent Antitumor Activity. *Mol. Cancer Ther.* **2021**, *20* (12), 2317−2328.
(8) Haque, T.; Cadenas, F. L.; Xicoy, B.; Alfonso, A.; Platzbecker, U.; Avivi, I.; Brunner, A. M.; Chromik, J.; Morillo, D.; Patel, M. R.; Falantes, J. F.; Leitch, H. A.; Germing, U.; Preis, M.; Lavie, D.; Lenox, L.; Lauring, J.; Kalota, A.; Brown, R.; Mehta, J.; Pastore, F.; Mistry, P.; Valcarcel, D. Phase 1 Study of JNJ-64619178, a Protein Arginine Methyltransferase 5 Inhibitor, in Patients with Lower-Risk Myelodysplastic Syndromes. *Blood* **2021**, *138* (Supplement 1), 2606.
(9) *A Phase 1, First-in-Human, Open-Label Study of the Safety, Pharmacokinetics, and Pharmacodynamics of JNJ-64619178, an Inhibitor of Protein Arginine Methyltransferase 5 (PRMT5) in Subjects With Advanced Cancers*. 2018
(10) Rodon, J.; Rodriguez, E.; Maitland, M. L.; Tsai, F. Y.; Socinski, M. A.; Berlin, J. D.; Thomas, J. S.; Al Baghdadi, T.; Wang, I. M.; Guo, C.; Golmakani, M.; Clark, L. N.; Gazdoiu, M.; Li, M.; Tolcher, A. W. A phase I study to evaluate the safety, pharmacokinetics, and pharmacodynamics of PF-06939999 (PRMT5 inhibitor) in patients with selected advanced or metastatic tumors with high incidence of splicing factor gene mutations. *ESMO Open* **2024**, *9* (4), 102961.
(11) Jensen-Pergakes, K.; Tatlock, J.; Maegley, K. A.; McAlpine, I. J.; McTigue, M.; Xie, T.; Dillon, C. P.; Wang, Y.; Yamazaki, S.; Spiegel, N.; Shi, M.; Nemeth, A.; Miller, N.; Hendrickson, E.; Lam, H.; Sherrill, J.; Chung, C. Y.; McMillan, E. A.; Bryant, S. K.; Palde, P.; Braganza, J.; Brooun, A.; Deng, Y. L.; Goshtasbi, V.; Kephart, S. E.; Kumpf, R. A.; Liu, W.; Patman, R. L.; Rui, E.; Scales, S.; Tran-Dube, M.; Wang, F.; Wythes, M.; Paul, T. A. SAM-Competitive PRMT5 Inhibitor PF-06939999 Demonstrates Antitumor Activity in Splicing Dysregulated NSCLC with Decreased Liability of Drug Resistance. *Mol. Cancer Ther.* **2022**, *21* (1), 3−15.
(12) *A Phase 1, Open-Label, Multicenter, Dose Escalation and Expansion Study of PRT811 in Subjects With Advanced Solid Tumors, CNS Lymphoma, and Recurrent High-Grade Gliomas*. 2019.
(13) *A Study of PRT543 in Participants With Advanced Solid Tumors and Hematologic Malignancies*. https://clinicaltrials.gov/ct2/show/NCT03886831 (accessed Jan 18).
(14) Yu, J.; Sun, Y.; Guo, S.; Wang, H.; Wu, J.; Jiang, X.; Chen, J.; Yang, G.; Yang, C. 675P A phase I study of safety, pharmacokinetics, and pharmacodynamics of SCR-6920, a protein arginine methyltransferase 5 (PRMT5) inhibitor, in patients with advanced malignant tumors. *Annals of Oncology* **2023**, *34*, S474.
(15) *A Phase I Study to Investigate the Safety, Tolerability, Preliminary Efficacy and Pharmacokinetics(PK) of SCR-6920 Capsule in Patients With Advanced Malignant Tumors*. 2022.
(16) Watts, J. M.; Bradley, T. J.; Thomassen, A.; Brunner, A. M.; Minden, M. D.; Papadantonakis, N.; Abedin, S.; Baines, A. J.; Barbash, O.; Gorman, S.; Kremer, B. E.; Borthakur, G. M. A Phase I/II Study to Investigate the Safety and Clinical Activity of the Protein Arginine Methyltransferase 5 Inhibitor GSK3326595 in Subjects with Myelodysplastic Syndrome and Acute Myeloid Leukemia. *Blood* **2019**, *134* (Supplement_1), 2656.
(17) *A Phase II Randomized Window of Opportunity Trial Evaluating Clinical and Biological Effects of PRMT5 Inhibitor, GSK3326595 in Early Stage Breast Cancer*. Ontario Institute for Cancer Reseaech, Hamilton Health Sciences, GlaxoSmithKline, London Regional Cancer Canada, 2020.
(18) Smith, C. R.; Aranda, R.; Christensen, J. G.; Engstrom, L. D.; Gunn, R. J.; Ivetac, A.; Ketcham, J. M.; Kuehler, J.; David Lawson, J.; Marx, M. A.; Olson, P.; Thomas, N. C.; Wang, X.; Waters, L. M.; Kulyk, S. Design and evaluation of achiral, non-atropisomeric 4-(aminomethyl)phthalazin-1(2H)-one derivatives as novel PRMT5/MTA inhibitors. *Bioorg. Med. Chem.* **2022**, *71*, 116947.
(19) Smith, C. R.; Aranda, R.; Bobinski, T. P.; Briere, D. M.; Burns, A. C.; Christensen, J. G.; Clarine, J.; Engstrom, L. D.; Gunn, R. J.; Ivetac, A.; Jean-Baptiste, R.; Ketcham, J. M.; Kobayashi, M.; Kuehler, J.; Kulyk, S.; Lawson, J. D.; Moya, K.; Olson, P.; Rahbaek, L.; Thomas, N. C.; Wang, X.; Waters, L. M.; Marx, M. A. Fragment-Based Discovery of MRTX1719, a Synthetic Lethal Inhibitor of the PRMT5*MTA Complex for the Treatment of MTAP-Deleted Cancers. *J. Med. Chem.* **2022**, *65* (3), 1749−1766.
(20) *A Phase 1/2 Multiple Expansion Cohort Trial of MRTX1719 in Patients With Advanced Solid Tumors With Homozygous MTAP Deletion*. 2022.
(21) Villalona-Calero, M. A.; Maki, R. G.; O'Neil, B.; Abbruzzese, J. L.; Dagogo-Jack, I.; Devarakonda, S.; Wahlroos, S.; Lin, C.-C.; Fujiwara, Y.; Terbuch, A.; Postel-Vinay, S.; Goebeler, M.-E.; Addeo, A.; Prenen, H.; Arkenau, T.; Sacher, A. G.; Liu, C.; Kormany, W.; Ahnert, J. R. Design and rationale of a phase 1 dose-escalation study of AMG 193, a methylthioadenosine (MTA)-cooperative PRMT5 inhibitor, in patients with advanced methylthioadenosine phosphorylase (MTAP)-null solid tumors. *J. Clin. Oncol.* **2022**, *40*, TPS3167.
(22) *A Phase 1/1b/2 Study Evaluating the Safety, Tolerability, Pharmacokinetics, Pharmacodynamics, and Efficacy of AMG 193 Alone and in Combination With Docetaxel in Subjects With Advanced MTAP-null Solid Tumors*. 2021.
(23) *A Phase 1b Study Evaluating the Safety, Tolerability, Pharmacokinetics, and Efficacy of AMG 193 Alone or in Combination With Other Therapies in Subjects With Advanced Thoracic Tumors With Homozygous MTAP-deletion (Master Protocol)*. 2024.
(24) *A Phase 1/2, Multi-Center, Open-Label Study to Evaluate the Safety, Tolerability, and Preliminary Antitumor Activity of TNG462 in Patients With MTAP-deleted Advanced or Metastatic Solid Tumors*. 2023.
(25) Briggs, K.; Tsai, A.; Zhang, M.; Tonini, M.; Haines, B.; Huang, A.; Cottrell, K. TNG462 is a potential best-in-class MTA-cooperative PRMT5 inhibitor for the treatment of peripheral MTAP-deleted solid tumors. *Eur. J. Cancer* **2022**, *174*, S84.
(26) Briggs, K.; Cottrell, K.; Tsai, A.; Zhang, M.; Tonini, M.; Yoda, S.; Lombardo, S.; Teng, T.; Davis, C.; Whittington, D.; DiBenedetto, H.; Huang, A.; Maxwell, J. TNG908 is a brain-penetrant, MTA-cooperative PRMT5 inhibitor for the treatment of MTAP-deleted cancer. *Eur. J. Cancer* **2022**, *174*, S84.
(27) *A Modular Phase I/II, Open-label, Multicentre Study to Evaluate the Safety, Tolerability, and Efficacy of AZD3470, a PRMT5 Inhibitor, as Monotherapy and in Combination With Anticancer Agent(s) in*

https://doi.org/10.1021/acsomega.4c08661
ACS Omega 2025, 10, 1156−1163

Participants With Relapsed/Refractory Haematologic Malignancies. 2023.
(28) *PRIMROSE: A Modular Phase I/IIa, Multicentre, Dose Escalation, and Expansion Study of AZD3470, a MTA Cooperative PRMT5 Inhibitor, as Monotherapy and in Combination With Anticancer Agents in Patients With Advanced/Metastatic Solid Tumours That Are MTAP Deficient*. 2023.
(29) McKinney, D. C.; McMillan, B. J.; Ranaghan, M. J.; Moroco, J. A.; Brousseau, M.; Mullin-Bernstein, Z.; O'Keefe, M.; McCarren, P.; Mesleh, M. F.; Mulvaney, K. M.; Robinson, F.; Singh, R.; Bajrami, B.; Wagner, F. F.; Hilgraf, R.; Drysdale, M. J.; Campbell, A. J.; Skepner, A.; Timm, D. E.; Porter, D.; Kaushik, V. K.; Sellers, W. R.; Ianari, A. Discovery of a First-in-Class Inhibitor of the PRMT5-Substrate Adaptor Interaction. *J. Med. Chem.* **2021**, *64* (15), 11148−11168.
(30) Mulvaney, K. M.; Blomquist, C.; Acharya, N.; Li, R.; Ranaghan, M. J.; O'Keefe, M.; Rodriguez, D. J.; Young, M. J.; Kesar, D.; Pal, D.; Stokes, M.; Nelson, A. J.; Jain, S. S.; Yang, A.; Mullin-Bernstein, Z.; Columbus, J.; Bozal, F. K.; Skepner, A.; Raymond, D.; LaRussa, S.; McKinney, D. C.; Freyzon, Y.; Baidi, Y.; Porter, D.; Aguirre, A. J.; Ianari, A.; McMillan, B.; Sellers, W. R. Molecular basis for substrate recruitment to the PRMT5 methylosome. *Mol. Cell* **2021**, *81* (17), 3481−3495 e7.
(31) Krzyzanowski, A.; Gasper, R.; Adihou, H.; Hart, P.; Waldmann, H. Biochemical Investigation of the Interaction of pICln, RioK1 and COPR5 with the PRMT5-MEP50 Complex. *Chembiochem* **2021**, *22* (11), 1908−1914.
(32) Krzyzanowski, A.; Esser, L. M.; Willaume, A.; Prudent, R.; Peter, C.; t Hart, P.; Waldmann, H. Development of Macrocyclic PRMT5-Adaptor Protein Interaction Inhibitors. *J. Med. Chem.* **2022**, *65* (22), 15300−15311.
(33) Beketova, E.; Fang, S.; Owens, J. L.; Liu, S.; Chen, X.; Zhang, Q.; Asberry, A. M.; Deng, X.; Malola, J.; Huang, J.; Li, C.; Pili, R.; Elzey, B. D.; Ratliff, T. L.; Wan, J.; Hu, C. D. Protein Arginine Methyltransferase 5 Promotes pICln-Dependent Androgen Receptor Transcription in Castration-Resistant Prostate Cancer. *Cancer Res.* **2020**, *80* (22), 4904−4917.
(34) Eberhardt, J.; Santos-Martins, D.; Tillack, A. F.; Forli, S. AutoDock Vina 1.2.0: New Docking Methods, Expanded Force Field, and Python Bindings. *J. Chem. Inf. Model.* **2021**, *61* (8), 3891−3898.
(35) Kim, H.; Lee, J.; Ahn, S.; Lee, J. R. A merged molecular representation learning for molecular properties prediction with a web-based service. *Sci. Rep.* **2021**, *11* (1), 11028.
(36) The Atomwise AIMS Program. AI is a viable alternative to high throughput screening: a 318-target study. *Sci. Rep.* **2024**, *14* (1), 7526.
(37) Azari, H.; Millette, S.; Ansari, S.; Rahman, M.; Deleyrolle, L. P.; Reynolds, B. A. Isolation and expansion of human glioblastoma multiforme tumor cells using the neurosphere assay. *J. Vis Exp* **2011**, No. e3633.
(38) Izadi, S.; Anandakrishnan, R.; Onufriev, A. V. Building Water Models: A Different Approach. *J. Phys. Chem. Lett.* **2014**, *5* (21), 3863−3871.
(39) Tian, C.; Kasavajhala, K.; Belfon, K. A. A.; Raguette, L.; Huang, H.; Migues, A. N.; Bickel, J.; Wang, Y.; Pincay, J.; Wu, Q.; Simmerling, C. ff19SB: Amino-Acid-Specific Protein Backbone Parameters Trained against Quantum Mechanics Energy Surfaces in Solution. *J. Chem. Theory Comput.* **2020**, *16* (1), 528−552.
(40) He, X.; Man, V. H.; Yang, W.; Lee, T. S.; Wang, J. A fast and high-quality charge model for the next generation general AMBER force field. *J. Chem. Phys.* **2020**, *153* (11), 114502.

https://doi.org/10.1021/acsomega.4c08661
ACS Omega 2025, 10, 1156−1163